



# AI-Driven Intelligent Medical System: Deep Learning for Chest X-Ray/CT Disease Recognition

Ahmed Saleh; Ahmed Sied; Rahma Gharib; Alaa Elsaid; Ahmed Mabrouk; Hoda El-Batrawy.

Faculty of Computer and Information Science, Damnhour University, Egypt.

**Abstract**— In the wake of the global health crisis, healthcare institutions, including hospitals, physicians, medical staff, and patients, faced an urgent need for an advanced medical management system to streamline operations and enhance diagnostic accuracy and efficiency. Consequently, the proposed intelligent medical Chest system (IMCS) leverages artificial intelligence (AI) and deep learning technologies to optimize workflows among healthcare professionals, enabling them to perform their duties more effectively and expedite patient diagnoses with greater precision. The system incorporates both low-dose computed tomography (CT) and chest radiography (CXR) for the screening of lung cancer. While CT offers superior diagnostic precision, it is accompanied by challenges in resource allocation and potential radiation risks. In contrast, CXR serves as a more cost-effective and resource-efficient preliminary screening modality. Leveraging advanced artificial intelligence (AI) and deep learning techniques, the system analyzes both imaging types, streamlining clinical workflows, augmenting diagnostic accuracy, and accelerating patient evaluation and management. By leveraging the sophisticated capabilities of both chest X-rays and CT scans, which each provide unique insights into tissue anomalies, the suggested model dramatically increases diagnostic precision. To efficiently handle and interpret the data from each imaging modality, the model is built on a complex convolutional neural network (CNN) architecture that includes numerous convolutional blocks and fully linked layers. With a classification accuracy of 98.9% for CT scans and 94.6% for X-rays, the system surpasses conventional manual and computerized methods, providing a more thorough and dependable approach for early disease detection and diagnosis.

**Keywords**—Chest CT, Image Pre-Processing, Optimization, Deep Learning, Cross-Entropy.

## 1. Introduction

Artificial intelligence (AI) has emerged as a key instrument for improving diagnosis and treatment in the medical industry [1]. AI-based medical systems can now identify and diagnose a wide range of illnesses by evaluating medical imaging data, including X-rays, CT scans, and MRIs, thanks to the use of deep learning algorithms and image analysis. By decreasing diagnostic errors, increasing the precision and speed of patient evaluations, and automating the interpretation of complicated imaging data, these technologies support medical personnel. By utilizing enormous volumes of medical data, AI can also spot trends that human practitioners would miss at first, allowing for earlier detection and more individualized treatment regimens.

Globally, lung cancer is regarded as a major health concern as it accounts for a large percentage of deaths related to cancer [2]. In most cases, lung cancer can be divided into two main types: non-small cell lung cancer (NSCLC) or large cell lung cancer (LCLC) and small cell lung cancer (SCLC), the most prevalent of which is NSCLC / LCLC. The most prevalent variety is NSCLC/LCLC. Although genetics, environmental exposure, and air pollution also put non-smokers at risk, smoking continues to be the predominant risk factor. It might be difficult to detect early-stage lung cancer since it frequently shows no symptoms. Due to this, a large number of cases are discovered when the cancer has

progressed, drastically lowering the number of available treatments and survival rates.

In this article, we concentrate on the diagnostic and detection capabilities of medical diseases through the utilization of both computed tomography (CT) scans [3] and X-rays [4]. CT, also referred to as computerized axial tomography (CAT), is a sophisticated imaging modality that employs X-rays to generate intricate three-dimensional representations of the internal anatomical structures of the human body. This advanced technology facilitates the precise understanding of tissue and organ configuration, thereby enabling accurate and efficient disease detection. One of the principal advantages of CT scans lies in their capacity to detect even the most minute alterations in tissues and organs, rendering them indispensable for early and precise diagnosis. Conversely, X-rays, while offering less granularity, are extensively utilized for initial diagnostic assessments and provide critical insights into the body's internal architecture, thereby assisting in the identification of conditions such as pulmonary infections or skeletal fractures.

The IMCS provides a comprehensive and effective approach to disease identification by utilizing both CT scans and X-rays. Even the smallest pathological changes that could indicate underlying medical issues can be detected thanks to CT scans, which make it easier to precisely assess internal tissue structures. In early diagnostic assessments, X-rays are crucial for identifying



anomalies such lung infections or skeletal fractures, even though they provide less detailed information. When taken as a whole, these imaging modalities improve patient outcomes and clinical decision-making by enhancing the diagnostic process.

Leveraging these imaging modalities independently, the system provides a multifaceted and precise instrument for diagnosing a spectrum of thoracic pathologies, facilitating enhanced early detection and advancing clinical decision-making in respiratory medicine. We augmented a deep learning (DL)-based model constructed upon a sophisticated convolutional neural network (CNN) architecture [5] meticulously calibrated for chest disease detection through the discrete application of CT scans and X-rays to refine diagnostic accuracy. For CT scans, the model is rigorously trained to discern specific pulmonary malignancies such as adenocarcinoma, large cell carcinoma, normal lung parenchyma, and squamous cell carcinoma [6], exploiting CT's advanced 3D imaging prowess to evaluate subtle morphological transformations. Distinctly, for X-ray images, the model is capable of identifying an expansive array of respiratory conditions, including atelectasis, consolidation, infiltration, pneumothorax, edema, emphysema, fibrosis, effusion, pneumonia, pleural thickening, cardiomegaly, nodules, masses, and hernia. The model was trained and validated on publicly accessible benchmark datasets, with strategic data augmentation applied to bolster the diversity of training data, thus refining the model's generalization capacity [7].

Logically, the paper has been separated into sections. In Section I, it was suggested that deep learning be used for CT scans and X-rays diagnosis. Section II covers previous research on the subject; Section III goes into detail about the system's methodology; Section IV is devoted to the collection of datasets; Sub-Section A illustrates the dataset's pre-processing methodology; and Sub-Section B displays the hyper-parameterization that was set prior to training. The suggested CNN architecture is displayed in Section V. A sequential model is shown in Section VI. A metric for evaluation is proposed in Section VII. Results and comparisons are given in Section VIII. In Section IX, the paper concludes with a projected analysis.

## **2. RELATED WORKS**

Extensive scholarly efforts have focused on using deep learning techniques to interpret CT scans and X-rays in order to improve diagnosis accuracy and operational efficiency in medical imaging. Convolutional neural networks (CNNs) and other advanced architectures are useful for the subtle diagnosis and classification of thoracic diseases, as this body of research demonstrates. Empirical research shows that deep learning not only improves diagnostic workflow accuracy but also makes it easier to identify serious illnesses like lung cancers early on and allows for careful monitoring of disease progression with no intervention from clinicians. The next chapter outlines the key developments and approaches that support this field, illuminating

significant research findings and their revolutionary effects on diagnostic radiology.

### **2.1 overview of related work concerning CT scans**

Al-Shouka et al. [8] CNN architecture were employed by researchers to construct a smart forecasting model for lung cancer [9,10]. Authors represented forward in this domain, harnessing the capabilities of CNNs to discern subtle patterns indicative of lung malignancies. The CNN's design consists of many layers convolutional subsequent to pooling and fully-linked. The way the model is able to capture intricate features to identify subtle anomalies that might elude human observers. Researchers have fine-tuned hyper-parameters, optimized loss functions [11], and employed techniques like data augmentation to enhance the model's robustness [12]. Python libraries such as Pandas, NumPy, and Matplotlib facilitate data preprocessing, exploration, and visualization. To ensure that subsets of data are allotted for training, validation, and testing, they first employed data splitting. When files are duplicated and organized properly, information is kept in the appropriate places for quick access during training models. Second, they used the CT-scan image collection to apply image preprocessing. They scaled the pixel values to the interval of [0, 1] by using image normalization, which divided the pixel values by 255. picture format that used JPG conversion to store and send massive amounts of image data. A brightness reduction occurs when the image resolution value is less than 1.0. sharpness of the image using the 2D function of cv2.filter. To change the resolution and noise level of the image, adjust the scale and noise reduction parameters. The pre-processed images increased the internal system's efficiency. With 86% accuracy, 91% precision, 92% recall, and 87% sensitivity, This method is more effective, precise, and quick than traditional techniques.

Mamun et al. [13] We suggested a deep learning model for the early diagnosis of lung cancer of a scan dataset of computed tomography (CT) based on CNN. In demand to study deep learning models for image identification or categorization, pre-processing technique was necessary. The images were pre-processed through adjusting the size them, noise reduction , segmentation techniques. The proposed CNN model outperformed other architectures, including Inception-V3, Xception, and ResNet-50 [14:18]. The optimization algorithm known as Adam had been applied to compile the model. The Keras Python module was used to obtain a loss function of cross-entropy as well as other measurements. The evaluation metrics demonstrate its effectiveness: 92% an accuracy, 98.21% an Area Under Curve (AUC), 91.72% a recall and 0.328 a loss . These results indicate the potential of this approach to significantly improve lung cancer diagnosis compared to traditional methods.

Siddiqui et al. [19] employed a multi-step approach to achieve accurate classification of CT scans. First and foremost, the researchers leveraged transfer knowledge of learning, a powerful technique that allows previously trained neural network models to be fine-tuned for a



specific task. In this case, they utilized pre-trained deep learning models, incorporates Inception-v3, DenseNet-121, Inception-ResNet-v2, and Resnet-50 [20,21]. These models were previously trained on ImageNet as a large-scale image datasets, enabling them to capture relevant features from medical images effectively. Data augmentation was also used prior to training; however, the results were not better. Ultimately, images in their original dimensions (299\*299 pixels) were trained using transfer learning. The effectiveness of the model has been assessed using metrics for performance. They introduced an ensemble learning paradigm rather than relying on a single model; the ensemble approach combined multiple deep learning architectures. Each of these models contributed its predictions, which were then aggregated to make a collective decision. By doing so, the researchers aimed to mitigate biases and improve overall robustness in classification. Its efficacy is demonstrated by the evaluation measures, which show 96% accuracy and a 96% f1 score. These findings suggest that, in comparison to conventional techniques, the assembled methodology has the potential to greatly enhance diagnosis of lung cancer diseases.

Raza et al. [22] suggested a brand-new Lung-EffNet is a predictive model based on learning from transfers. Lung-EffNet is constructed around the EfficientNet architecture, with additional layers added to the model's classification head. EfficientNet is used in five different forms to evaluate Lung-EffNet. They used EfficientNetB1 and transfer learning to provide a fine-tuning method for classifying lung cancer from CT scan pictures [23]. To efficiently extract pertinent characteristics from lung cancer CT scan pictures, EfficientNetB1 has been fine-tuned. The experimental outcomes highlight the positive outcomes of the suggested approach. In terms of efficiency of the model, EfficientNetB1 continuously beats existing CNN architectures. It achieves an astounding accuracy of 98.5% and shows strong ROC scores on test sets, ranging from 97% to 99%. These findings demonstrate EfficientNetB1's potential as an effective tool for automated lung cancer categorization and diagnosis. Increasing the quantity of the dataset would improve the suggested approach's generalizability and confirm its efficacy in real-world situations. With regard to the anticipated outcomes, Lung-EffNet, which is based on Efficient-Net-B1, outperforms all other CNN. This makes it a realistic choice for automated lung cancer diagnosis from CT scan images, and a good possibility for widespread clinical application

## 2.2 overview of related work concerning X-rays.

Sharad J.D. al. [24] leverages an enhanced U-Net architecture with a classification layer to improve image segmentation and classification tasks, specifically for thoracic disease detection from chest X-ray images using the NIH Chest X-Ray Dataset. The U-Net framework, featuring an encoder for high-level feature extraction and a decoder for segmented output reconstruction, incorporates skip connections to achieve precise

localization by combining low-level and high-level features. Integrating a classification layer enables the model to not only segment regions but also classify them into specific categories, providing detailed insights into image content. The model is further enhanced with residual blocks to improve feature extraction and data augmentation techniques to increase robustness. Optimized using the Adam optimizer, which adapts learning rates based on gradient moments, and a cross-entropy loss function, the model achieves superior segmentation and classification performance. Binary accuracy and macro-accuracy are employed to handle imbalanced multi-class datasets effectively, demonstrating the system's robustness. Binary accuracy measures the proportion of correct predictions, with values ranging from 0 to 1, where 1 indicates perfect accuracy. Training binary accuracy starts at 0.9074 in epoch 1 and generally improves, reaching 0.9281 by epoch 16, indicating the model's enhanced ability to classify training data accurately. Validation binary accuracy starts at 0.9216 in epoch 1 and increases to a peak of 0.9302 by epoch 15, reflecting the model's effectiveness on unseen data. This approach showcases significant potential in aiding medical professionals with accurate and efficient thoracic disease diagnosis. Future work will focus on optimizing architectures, fine-tuning hyperparameters, and incorporating additional clinical data to enhance scalability, accuracy, and generalizability across larger datasets.

Mana Saleh Al Reshan et al. [25] proposed a deep learning-based model for distinguishing between mild and severe pneumonia patients is presented. The study uses two different datasets—one with 5,856 chest X-ray pictures and another with 112,120 images from 30,085 people, ChestX-ray14—to assess eight pre-trained models: ResNet50, ResNet152V2, DenseNet121, DenseNet201, Xception, VGG16, EfficientNet, and MobileNet. The MobileNet model produced the best classification results, with accuracies of 94.23% and 93.75% on the two datasets. For reliable model performance, important hyperparameters such as batch size, epoch count, and optimization techniques were carefully considered. The study shows that among the pre-trained models, MobileNet showed the highest accuracy thanks to its lightweight architecture and unique convolution layers. With the help of professional validation and data augmentation, this strategy has encouraging potential to help with early pneumonia.

Adel Sulaiman et al. [26] leverages a concatenate block equipped with advanced filters to extract crucial image features, while incorporating a transpose layer to augment the spatial resolution of the resultant feature maps. Trained using k-fold cross-validation (k=5), the model ensures optimal performance across five distinct subsets of the dataset. The dataset comprises 704 training and 96 testing chest X-ray (CXR) images, each coupled with corresponding masks and clinical annotations. This structured format, augmented by the precision of the masks, enables meticulous segmentation of lung tissue and enhances the accuracy of disease classification. The training process is fine-tuned with hyperparameters such





as a batch size of 32, the Adam optimizer for efficient gradient descent, and a total of 40 epochs to ensure robust learning and generalization. The suggested CNN model produced a 97% accuracy rate with very little loss. This model is constrained by several limitations, including a restricted range of disease categories, a limited dataset, and the risk of overfitting. These factors hinder its ability to generalize effectively across a broader spectrum of medical conditions and diverse patient populations.

Marriam Nawaz et al. [27] introduced the CXray-EffDet model, a deep learning-based framework for detecting and classifying chest diseases from X-ray images, addressing challenges such as structural complexities, image artifacts, and inter-/intra-class similarities. Leveraging the EfficientNet-B0-based EfficientDet-D0 architecture [28], the model effectively extracts features and performs classification across eight chest disease categories. Evaluated on the NIH CXR database, it achieved a mean Average Precision (mAP) score of 0.926, with precision and recall rates of 90% and 92.36%, respectively, outperforming peer approaches by 19.40% in mAP and demonstrating a minimum execution time of 0.20 seconds. The results highlight the model’s robustness in handling image distortions and its proficiency in precise localization and classification, offering a reliable tool for aiding medical professionals in diagnosing chest abnormalities.

### 3. Application Model

We have engineered a sophisticated IMCS, hosted on web servers, designed to augment the diagnostic capabilities of healthcare practitioners by accelerating the decision-making process. The system leverages cutting-edge deep learning algorithms, particularly for the analysis of medical imagery, enabling the precise identification and diagnosis of various pathologies. Through its advanced image processing and classification capabilities, this system empowers clinicians to obtain rapid and reliable diagnostic insights, thereby enhancing clinical efficiency and improving patient outcomes.

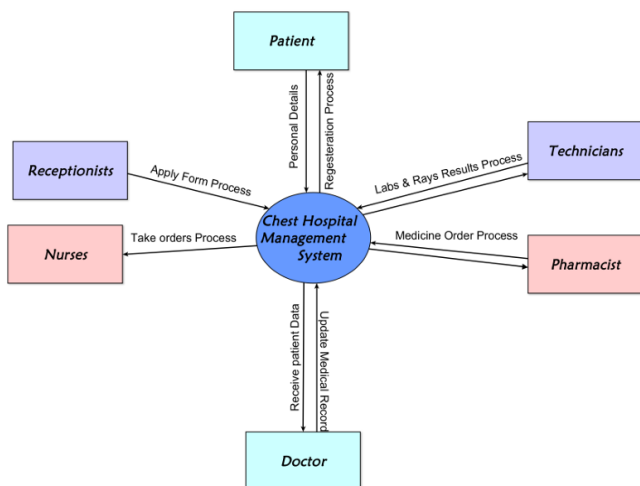


Figure 1. IMCS Context Diagram

### 3.1 Data Sources

In Figure 1, the context diagram of our intelligent chest hospital system, the central entity, denoted as the ‘Chest Hospital,’ represents the nucleus of the system’s operations. Surrounding this are six principal entities: ‘Patients,’ ‘Physicians,’ ‘Receptionists,’ ‘Pharmacists,’ ‘Technicians,’ and ‘Nurses.’ Each entity is interconnected with the hospital through bidirectional flows, indicating the reciprocal and continuous exchange of critical data. Patients submit personal and clinical information and receive health guidance, while Physicians contribute diagnostic insights and access patient records. The Receptionist facilitates administrative processes, the Pharmacist orchestrates pharmaceutical orders, the Technician oversees imaging and laboratory outcomes, and the Nurse administers directives. This diagram captures the comprehensive communicative architecture essential to the system’s operational efficacy.

The datasets employed in this study are meticulously curated from the Kaggle archive, encompassing a comprehensive collection of medical imaging data from both chest X-rays and CT scans, integral for the training and validation of advanced deep learning models aimed at pulmonary disease prediction.

### 3.2 X-ray image analysis

We leveraged the expansive National Institutes of Health (NIH) Chest X-ray Dataset, which comprises 112,120 X-ray images sourced from 30,805 unique patients [29]. This robust dataset is annotated with a diverse array of disease labels, including Atelectasis, Consolidation, Infiltration, Pneumothorax, Edema, Emphysema, Fibrosis, Effusion, Pneumonia, Pleural Thickening, Cardiomegaly, Nodule/Mass, Hernia, and a ‘No findings’ category (normal). These labels were derived using Natural Language Processing (NLP) techniques to extract relevant disease classifications from accompanying radiological reports, rendering this dataset an exemplary resource for developing deep learning models to enhance diagnostic accuracy and assist clinicians in detecting pulmonary diseases.

### 3.3 CT Scans image analysis

With a focus on lung cancer, the `NTI_cnn_ct` dataset from Kaggle was used for the CT scan analysis. This collection includes high-resolution photos with thorough annotations for a number of cancer kinds, such as squamous cell carcinoma, large cell carcinoma, adenocarcinoma, and normal. By arranging these images into training, testing, and validation sets, a thorough foundation for developing models that can identify and categorize various types of lung cancer is created. The capacity of the model to recognize intricate patterns and correctly identify lung cancer from CT scan images depends on the comprehensive annotations and high-quality imaging data. The CT scan images used in this lung cancer dataset were gathered from the openly accessible "Kaggle" web resource [30]. There are 967 images in CT scan dataset, which are separated into three



subsets of data. 613 images for the training set, the 315 images for validation set, and 72 images for the testset . Each category is divided evenly across its four classes

#### 4. Model Framework Development

This analytical framework initiates with a publicly accessible, meticulously curated image repository, consisting of chest X-ray and CT scan images procured from open-access websites. A rigorous pre-processing phase is implemented across the entire dataset, enhancing image quality and standardizing dimensions to optimize input compatibility with deep learning techniques. The proposed models, developed as Convolutional Neural Networks (CNNs) with sequential architectures, undergo systematic testing, training, and validation using a conventional hold-out validation protocol to ensure model reliability and generalizability across various data partitions [31,32].

Each CNN model leverages a sophisticated architecture, comprising a series of intricately layered convolutional blocks and dense fully connected layers. These blocks are crafted to capture complex spatial hierarchies and minute structural distinctions inherent in pulmonary imaging. Through this design, the models achieve precise categorization of normal (non-cancerous) lung structures and diverse cancer phenotypes, including adenocarcinoma, large cell carcinoma, and squamous cell carcinoma.

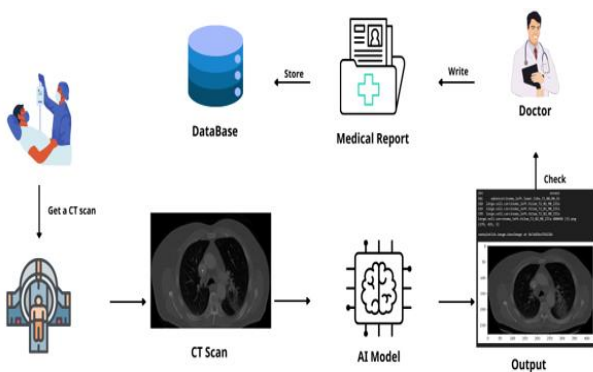


Figure 2. IMCS Framework

As illustrated in Fig. 1, the models’ input layers are configured to accommodate multi-dimensional CT and X-ray images, enhancing versatility and scaling capabilities. This structural design, paired with robust feature extraction mechanisms, enables refined classification capabilities, ensuring that even subtle morphological variations associated with various cancer types are accurately identified and distinguished within both chest CT scans and X-ray images. The proposed CNN models thus offer a comprehensive diagnostic tool, designed to assist in the nuanced classification and early detection of complex pulmonary conditions

#### 4.1 Dataset Preparation and Enhancement

To evaluate the model for image detection or classification, an effective pre-processing system is essential. Feature extraction plays a crucial role in preparing images by reading, resizing, segmenting,

denoising, and applying morphological transformations. Our system conducts multiple pre-processing tasks, including data splitting and augmentation. Augmentation enhances the dataset by generating varied samples through random transformations like rotation and flipping. Effective pre-processing allows the network to learn relevant features and improves model performance. Model accuracy over training epochs is visualized by plotting validation and training accuracy, illustrating how pre-processing influences learning and convergence across time.

#### 4.2 Model Optimization and Tuning

Optimization is crucial in neural network training, aiming to find the optimal model parameters (weights and biases) that minimize the loss function. Common optimization algorithms like Stochastic Gradient Descent (SGD) [33], Adam, and RMSProp iteratively update parameters based on gradients, accelerating convergence, helping escape local minima, and enhancing overall model performance. Choosing the right optimization method is essential for effective training.

For the first proposed sequential CNN models based on CT images, The images undergo meticulous pre-processing to ensure consistency and compatibility with the model, initiating with rescaling to normalize pixel values within the range of 0 to 1. This standardization technique is critical for enhancing model training and optimizing performance. Further pre-processing operations, such as normalization to adjust pixel values’ mean and standard deviation, alongside advanced augmentation techniques like rotation, shearing, and flipping, are strategically employed to bolster the model’s capacity to discern pertinent features and augment its generalization potential. Prior to training on the CT scan dataset, comprehensive hyper-parameter tuning is conducted, including setting the batch size to 64, adjusting image dimensions to 224 x 224, and configuring training to span 100 epochs. The model utilizes ReLU activation functions for hidden layers, SoftMax for classification, and a learning rate of 0.001 with the Adam optimizer to optimize convergence and accelerate learning efficacy [34].

For the second proposed model based on X-ray Image, with the dataset splits ready, we use Keras’s ImageDataGenerator to streamline preprocessing and augmentation. This generator not only facilitates image creation from a data frame but also includes features like standardization and augmentation. For normalization, samplewise\_center and samplewise\_std\_normalization were employed with True to adjust each sample to have a mean of zero and a standard deviation of one, ensuring consistent input distributions for training. Additionally, it applies augmentations such as slight shearing (shear\_range = 0.1), zooming (zoom\_range = 0.15), rotation (rotation\_range=5), and shifts in width and height (width\_shift\_range = 0.1, height\_shift\_range = 0.05). Horizontal flipping (horizontal\_flip=True) is also enabled to enhance variability, while vertical flipping



(vertical\_flip=False) is avoided as it is less meaningful for X-ray data. The fill\_mode='reflect' ensures that augmented areas are filled appropriately to prevent distortion. We also normalize the test and validation data using the mean and standard deviation computed from the training dataset to ensure fairness. To avoid computational expense, these statistics are approximated from a random sample, ensuring a balance between efficiency and accuracy. This approach guarantees fair and reliable model evaluation.

### 4.3 Impact Class Imbalance on Cross-Entropy.

This plot shows that there is a significant difference in the prevalence of positive cases across the different pathologies, and these trends reflect the distribution of positive cases across the entire dataset.

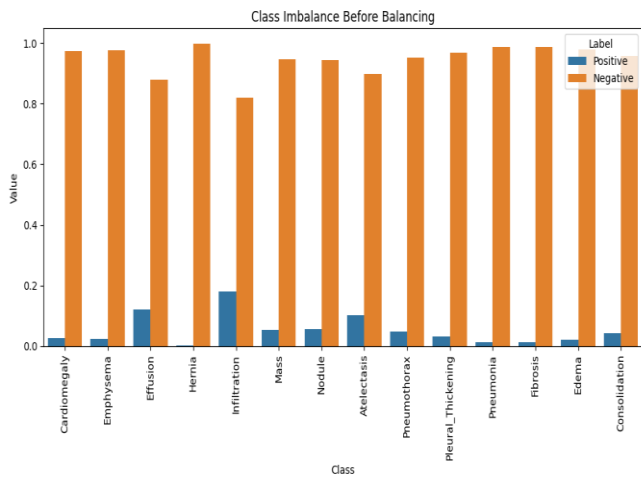


Figure 3. Class Imbalance before Balancing

A perfect training dataset would be one where both positive and negative training cases contribute equally to the overall loss when we train our model. The problem is, when using a standard cross-entropy loss function with such a highly imbalanced dataset, as shown here, the model will be incentivized to prioritize the majority class (i.e., the negative cases), since this class contributes to the overall loss more than any other class. Class imbalance presents a significant challenge when training machine learning models, especially with the cross-entropy loss function. We can rewrite the overall average cross-entropy loss over the entire training set  $D$  of size  $N$  as:

$$L_{CE}(D) = -\frac{1}{N} \left( \sum_{pe} \log(f(x_i)) + \sum_{ne} \log(1 - f(x_i)) \right)$$

In the case of a large class imbalance, the loss function is dominated by the majority class, with the minority class's contribution being minimal, leading to biased model performance. Using this formulation, we can see that the contribution of each class (i.e. positive or negative) is:

$$freq_p = \frac{n. of\ positive\ Ex}{N}$$

$$freq_n = \frac{n. of\ Negative\ Ex}{N}$$

As shown in the plot above, the contributions of positive cases are much lower than those of the negative ones. To

equalize these contributions, one approach is to multiply each example from each class by a class-specific weight factor, ensuring that the overall contribution of each class is balanced. This way will be balancing the contribution of positive and negative labels.

$$w_p \times freq_p = w_n \times freq_n$$

$$w_p = freq_n, w_n = freq_p$$

After computing the weights, the final weighted loss for each training case ensures that the positive and negative labels within each class contribute equally to the loss function.

$$L_{CE}^w(x) = -(w_p y \log(f(x)) + w_n (1 - y) \log(1 - f(x))).$$

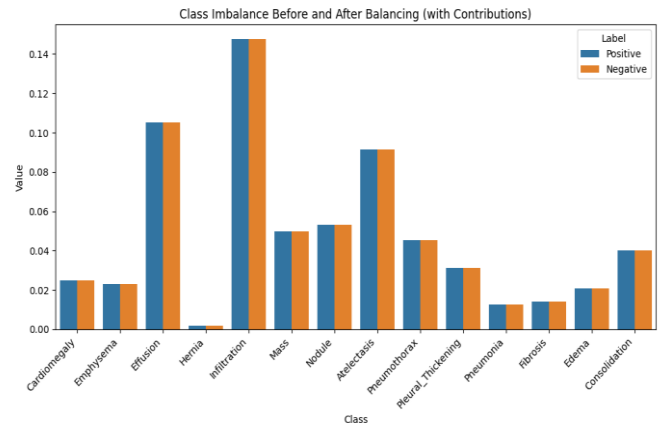


Figure 4. Class Imbalance After Balancing

## 5. PROPOSED CNN ARCHITECTURE

This system centers on leveraging the advanced capabilities of artificial intelligence, specifically through sophisticated machine learning and deep learning methodologies, to engineer a diagnostic framework meticulously designed for a pulmonary healthcare facility. In this study we employed two distinct models, each applied to a separate dataset.

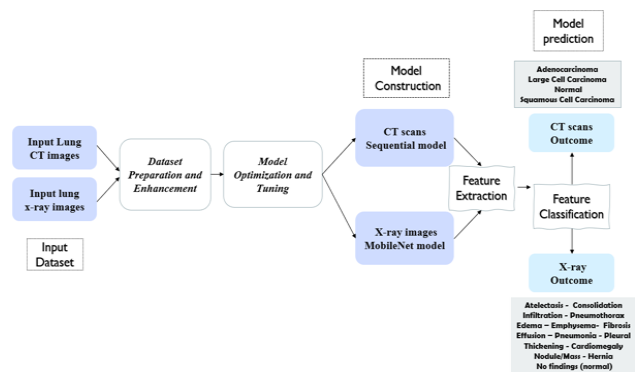


Figure 5. Architecture of IMCS Process

In the primary model, we leveraged the sequential model—a pivotal component within the Keras framework—to construct an advanced deep convolutional neural network (CNN) for lung cancer prognostication. This sequential architecture offers a streamlined methodology for formulating neural networks through the systematic layering of components,





making it particularly suitable for CNN configurations. In the second model, we will utilize the DenseNet121 model from the Keras Applications package and load the pretrained weights. Afterward, we will evaluate the model's performance by analyzing the ROC curve and AUROC values for the various diagnostic categories.

### 5.1 SEQUENTIAL MODEL

This study delineates the development of a sophisticated deep learning model utilizing the Keras Sequential API for the prognostication of lung cancer from CT images. The model harnesses the power of a convolutional neural network (CNN) architecture meticulously engineered to extract intricate, hierarchical features from medical imaging data, thereby enabling precise cancer classification. Fig.6 show the model's framework incorporates a series of convolutional blocks, strategically designed to optimize feature extraction and stabilize the training process. Batch normalization layers contribute to the acceleration of convergence and overall stability during the training phase, while dropout layers are integrated to mitigate overfitting and bolster generalizability. The final layer of the model employs a softmax activation function, tailored for multi-class classification, ensuring that output values represent a probabilistic distribution across four diagnostic categories [35]. The architecture is designed to progressively capture both low- and high-level features, making it an efficacious tool for the accurate and efficient diagnosis.

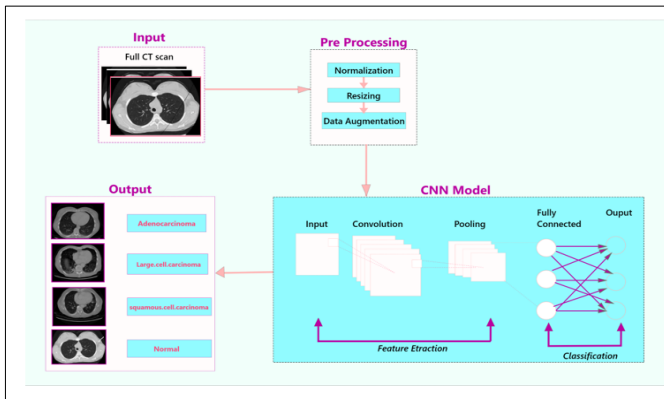


Figure 6. The Sequential CNN Model

**Block 1:** Pairs of layers of convolution with 64 filters, each constitute the first convolutional block. Batch normalization and max-pooling come next.

**Block 2:** The second block adds two convolutional layers with a total of 128 filters to the feature extraction procedure. Max-pooling and batch normalization are then performed.

**Block 3:** After learning more detailed feature representations, the third block has two convolutional layers of 256 filters. Each of them is followed by batch normalization and max-pooling.

**Block 4:** The last convolutional block improves feature representation even more by using three

convolutional layers, each with 512 filters, to make it easier to extract discriminative features.

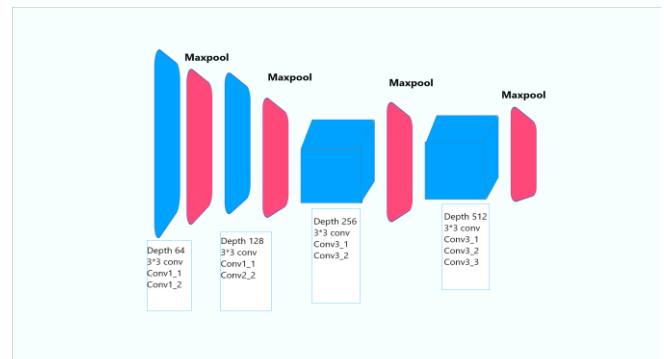


Figure 7. CNN Blocks of Sequential Model

A feature map generated undergoes a flattening transformation before traversing a fully connected 64-layer network that mirrors the convolutional architecture. This operation serves to facilitate feature synthesis and dimensionality reduction, enhancing the model's interpretability and computational efficiency. During training, a dropout layer with a rate of 0.25 is applied, randomly omitting 25% of the units to mitigate the risk of overfitting and bolster model generalization. The model culminates in an output layer comprising a dense layer with softmax activation, yielding probabilistic outputs across each classification category adenocarcinoma, large cell carcinoma, squamous cell carcinoma, and normal CT scan enabling nuanced categorization based on the input imaging data. Fig. 7 illustrates the four blocks of the sequentially proposed model.

In this study, the training regimen spans 50 epochs, ensuring thorough model convergence and optimization of performance. To fortify the model's resilience, data augmentation is applied, enriching the variability within the training dataset. The Adam optimizer, paired with the categorical cross-entropy loss function, is employed for multi-class classification, as both are commonly used and highly effective for such tasks. After defining the model architecture, these elements are assembled, and the model's accuracy is tracked to gauge performance during training.

### 5.2 Customized model built on EffcientNetB1

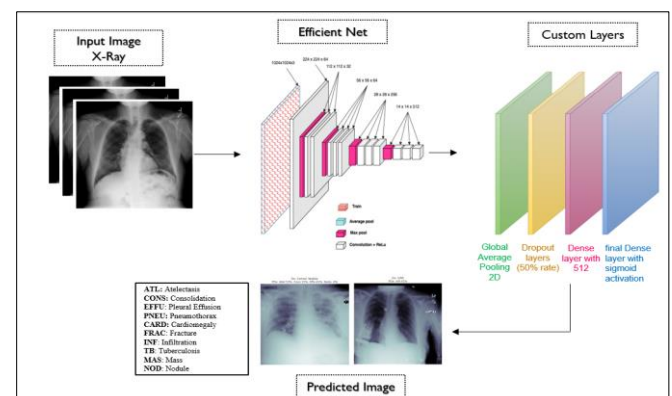


Figure 8. The Customized Model



The CustomNet121 model is designed with an input layer that accepts images of shape (224, 224, 3), or alternatively (128, 128, 3) as specified. The architecture begins with a 7x7 convolutional layer with 64 filters, followed by batch normalization, ReLU activation, and max-pooling. The model then proceeds through several dense blocks, which are sequentially stacked as per the num\_blocks parameter, specifying the number of layers in each block (e.g., [6, 12, 24, 16] for four blocks). Transition blocks are inserted after each dense block (except the last one) to reduce the number of features. The output layer applies batch normalization, ReLU activation, and global average pooling, followed by a final dense layer with num\_classes units and a softmax activation for classification. During model compilation, the Adam optimizer is used with a learning rate of 1e-4 and amsgrad = False. The model uses a custom weighted loss function, get\_weighted\_loss (pos\_weights, neg\_weights), ensuring balanced loss between positive and negative classes, and binary accuracy is employed as the evaluation metric.

power of AI-driven medical systems to enhance diagnostic accuracy, streamline clinical workflows, and ultimately improve patient outcomes through early and precise disease detection. Experts assess a classification model's efficacy using performance measures for categorization include F1-score, accuracy, precision, and recall [39,40].

## 6. RESULTS and COMPARISON

The integration of advanced deep learning models, such as the sequential CNNs and Customized model architectures, has proven highly effective for the classification and recognition of chest CT and X-ray images. Remarkably, the sequential CNNs attain accuracy of 98.9%, surpassing previous state-of-the-art of classification. The customized model build based on EffcientNetB1, meanwhile, has demonstrated the ability to analyze X-ray images in an efficient and accurate manner, having been able to achieve an outstanding 94.6% accuracy and have been able to accurately identify 14 pathological conditions with high performance. This two-part series of AI-driven models demonstrates the

### 6.1 CT Scan Analysis with Sequential Models.

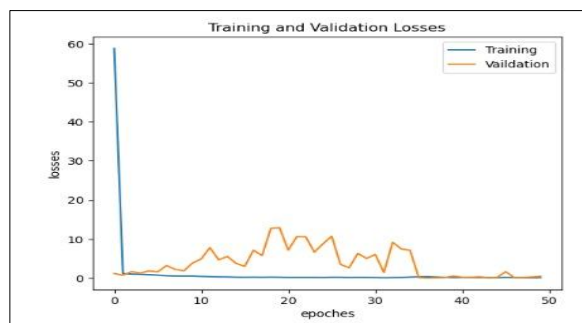


Figure 9. Training and Validation Loss



Figure 10. Training and Validation Accuracy

Table 1. Comparison proposed Sequential model with previous studies

Ref	Method	Performance Metric			
		Accuracy	Precision	Recall	F1-Score
[5]	CNN	86%	91%	92%	87%
[10]	CNN	92%	-----	91.7%	-----
[16]	Ensemble on pretrained models	96%	97%	99%	96%
[19]	Transfer Learning CNN	98.5%	100%	98.5%	99.1%
Proposed Model	Sequential CNN	98.9%	100%	98.9%	99.3%

### 6.2 X-Ray Analysis with Customized model

The customized model ensures faster diagnostics and helps in the effective detection of diseases. By fine-tuning EffcientNetB1.

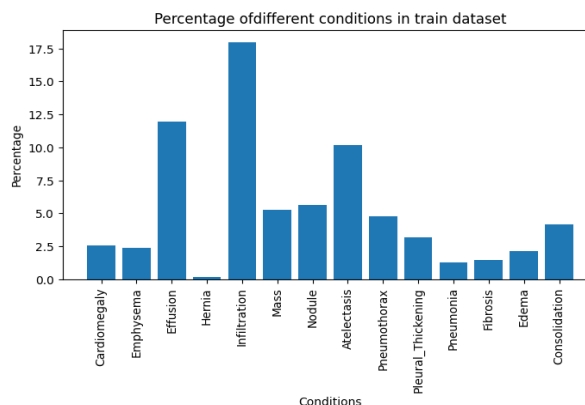


Figure 11. Distribution of Common Findings in X-Ray Image.



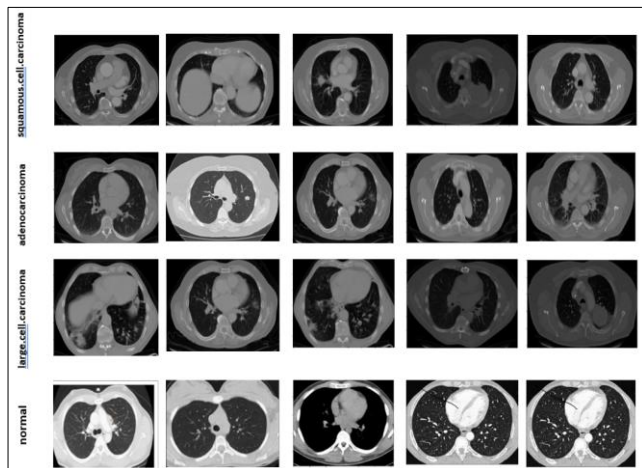


Figure 12.X-Ray Images after classification.

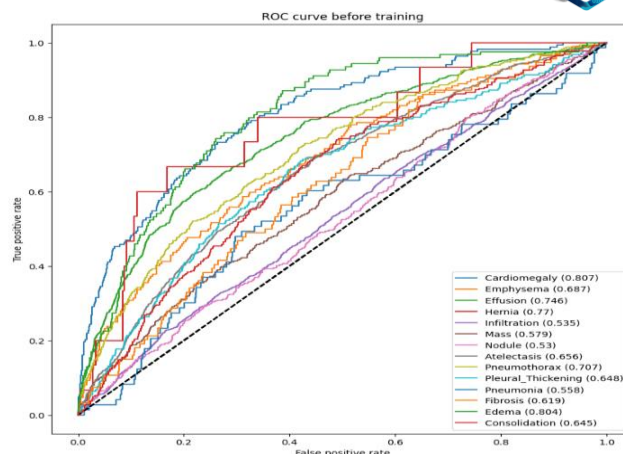
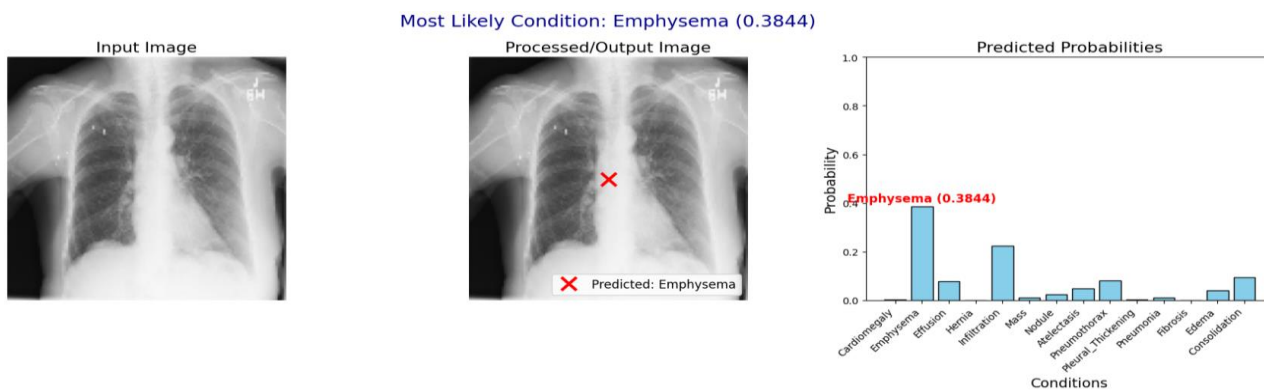


Figure 13.ROC Curve Analysis of Medical Condition.

Table 2. Comparison proposed Customized model built on EffcientNetB1 with previous studies

Ref	Method	Performance Metric		
		Accuracy	Precision	Recall
[28] 2023	CXray-EffDet	92.6%	90%	92.36%
[26] 2023	Lightweight Architecture based on MobileNet	93.75%	91.36%	94.39%
[24] 2023	Enhancing Thoracic Disease Diagnosis with U-Net	92.9 %	-----	-----
Proposed Model	Customized model built on EffcientNetB1	94.6%	93.3%	95.8%



### 7. CONCLUSION

This research presents a two deep CNNs, sequential deep learning and Customized model built on EffcientNetB1 for the classification of chest cancer types based on CT scan and X-Ray images. Through meticulous experimentation, we achieve exceptional accuracy levels, significantly surpassing previous benchmarks. The proposed IMCS is a system with software application based on AI that is installed on web servers to help medical professionals carry out their duties and diagnose patients more quickly and easily. One of the characteristics of this system is its ability for disease diagnosis effectively. The proposed model ultimately improving patient outcomes in the management of chest cancer. By exporting significant traits, grouping, and classifying them. An accuracy rating of sequential model

close to 99% and an accuracy for Customized model close to 95% . The proposed model feasible to predict whether a patient will get the disease or not.

### 8. REFERENCES

- [1] S. S. Rao, C. Rao, and S. Krantz, Artificial intelligence. Elsevier, 2023.
- [2] A. B. Rueschhoff, A. W. Moore, and M. R. P. Jasahui, "Lung Cancer Staging—A Clinical Practice Review," *Journal of Respiration*, vol. 4, no. 1, pp. 50-61, 2024
- [3] Seeram, "Computed Tomography: A Technical Review," *Dose Optimization in Digital Radiography and Computed Tomography: An Essential Guide*, pp. 41-56, 2023.



- [4] E. Çağlı, E. Sogancioglu, B. van Ginneken, K. G. van Leeuwen, and K. Murphy, "Deep learning for chest X-ray analysis: A survey," *Medical Image Analysis*, vol. 72, p. 102125, 2021.
- [5] L. Alzubaidi et al., "Review of deep learning: concepts, CNN architectures, challenges, applications, future directions," *Journal of big Data*, vol. 8, pp. 1-74, 2021.
- [6] J. Kim, H. Lee, and B. W. Huang, "Lung cancer: diagnosis, treatment principles, and screening," *American family physician*, vol. 105, no. 5, pp. 487-494, 2022.
- [7] S. K. Zhou, H. Greenspan, and D. Shen, *Deep learning for medical image analysis*. Academic Press, 2023.
- [8] R. Leluc, "Monte Carlo Methods and Stochastic Approximation: Theory and Applications to Machine Learning," Institut Polytechnique de Paris, 2023.
- [9] T. T. Al-Shouka and K. M. A. Alheeti, "Lung Cancer Intelligent Prediction System Using CNN," in *2023 International Conference on Decision Aid Sciences and Applications (DASA)*, 2023: IEEE, pp. 547-552.
- [10] B. T. Hammad, N. Jamil, I. T. Ahmed, Z. M. Zain, and S. Basheer, "Robust malware family classification using effective features and classifiers," *Applied Sciences*, vol. 12, no. 15, p. 7877, 2022.
- [11] C. Haarbarger, P. Weitz, O. Rippel, and D. Merhof, "Image-based survival prediction for lung cancer patients using CNNs," in *2019 IEEE 16th International Symposium on Biomedical Imaging (ISBI 2019)*, 2019: IEEE, pp. 1197-1201.
- [12] H. Naseri and V. Mehrdad, "Novel CNN with investigation on accuracy by modifying stride, padding, kernel size and filter numbers," *Multimedia Tools and Applications*, vol. 82, no. 15, pp. 23673-23691, 2023.
- [13] S. Yang, W. Xiao, M. Zhang, S. Guo, J. Zhao, and F. Shen, "Image data augmentation for deep learning: A survey," *arXiv preprint arXiv:2204.08610*, 2022.
- [14] M. Mamun, M. I. Mahmud, M. Meherin, and A. Abdelgawad, "Lcdctcnn: Lung cancer diagnosis of ct scan images using cnn based model," in *2023 10th International Conference on Signal Processing and Integrated Networks (SPIN)*, 2023: IEEE, pp. 205-212.
- [15] K. Simonyan and A. Zisserman, "Very Deep Convolutional Networks for Large-Scale Image Recognition." *arXiv*, Apr. 10, 2015. doi: 10.48550/arXiv.1409.1556, 2023.
- [16] O. Russakovsky et al., "Imagenet large scale visual recognition challenge," *International journal of computer vision*, vol. 115, pp. 211-252, 2015.
- [17] M. I. Mahmud, M. Mamun, and A. Abdelgawad, "A deep analysis of transfer learning-based breast cancer detection using histopathology images," in *2023 10th International Conference on Signal Processing and Integrated Networks (SPIN)*, 2023: IEEE, pp. 198-204.
- [18] M. I. Mahmud, M. Mamun, and A. Abdelgawad, "A deep analysis of textual features based cyberbullying detection using machine learning," in *2022 IEEE Global Conference on Artificial Intelligence and Internet of Things (GCAIoT)*, 2022: IEEE, pp. 166-170.
- [19] J. Miah, M. Mamun, M. M. Rahman, M. I. Mahmud, S. Ahmed, and M. H. B. Nasir, "MHfit: Mobile Health Data for Predicting Athletics Fitness Using Machine Learning," *arXiv preprint arXiv:2304.04839*, 2023.
- [20] S. A. Siddiqui, N. Fatima, and A. Ahmad, "Chest X-ray and CT scan classification using ensemble learning through transfer learning," *EAI Endorsed Transactions on Scalable Information Systems*, vol. 9, no. 6, pp. e8-e8, 2022.
- [21] C. Szegedy, S. Ioffe, V. Vanhoucke, and A. Alemi, "Inception-v4, inception-resnet and the impact of residual connections on learning," in *Proceedings of the AAAI conference on artificial intelligence*, 2017, vol. 31, no. 1.
- [22] G. Huang, Z. Liu, L. Van Der Maaten, and K. Q. Weinberger, "Densely connected convolutional networks," in *Proceedings of the IEEE conference on computer vision and pattern recognition*, 2017, pp. 4700-4708.
- [23] M. Mamun, A. Farjana, M. Al Mamun, and M. S. Ahammed, "Lung cancer prediction model using ensemble learning techniques and a systematic review analysis," in *2022 IEEE World AI IoT Congress (AIIoT)*, 2022: IEEE, pp. 187-193.
- [24] S.J. Dobariya "CLASSIFICATION OF THORAX DISEASES FROM CHEST X-RAY IMAGES CLASSIFIC," in *CSUSB ScholarWorks CSUSB ScholarWorks*, 2023.
- [25] M. S. A. Reshan et al., "Detection of pneumonia from chest X-ray images utilizing mobilenet model," in *Healthcare*, 2023, vol. 11, no. 11: MDPI, p. 1561.
- [26] A. Sulaiman et al., "A convolutional neural network architecture for segmentation of lung diseases using chest X-ray images," *Diagnostics*, vol. 13, no. 9, p. 1651, 2023.
- [27] M. Nawaz, T. Nazir, J. Baili, M. A. Khan, Y. J. Kim, and J.-H. Cha, "CXray-EffDet: chest disease detection and classification from X-ray images using the EfficientDet model," *Diagnostics*, vol. 13, no. 2, p. 248, 2023.
- [28] M. Tan, R. Pang, and Q. V. Le, "Efficientdet: Scalable and efficient object detection," in *Proceedings of the IEEE/CVF conference on computer vision and pattern recognition*, 2020, pp. 10781-10790.
- [29] R. Summers, "Nih chest x-ray dataset of 14 common thorax disease categories," NIH Clinical Center: Bethesda, MD, USA, 2019.
- [30] M. Hany, "Chest CT-Scan images Dataset. 2020," ed: Accessed, 2022.



- [31] R. Kumar, P. Kumbharkar, S. Vanam, and S. Sharma, "Medical images classification using deep learning: a survey," *Multimedia Tools and Applications*, vol. 83, no. 7, pp. 19683-19728, 2024.
- [32] M. Tan and Q. Le, "Efficientnet: Rethinking model scaling for convolutional neural networks," in *International conference on machine learning*, 2019: PMLR, pp. 6105-6114.
- [33] A. F. Agarap, "Deep learning using rectified linear units (relu)," *arXiv preprint arXiv:1803.08375*, 2018.
- [34] G. Lan, *First-order and stochastic optimization methods for machine learning*. Springer, 2020.
- [35] A. D. Rasamoelina, F. Adjailia, and P. Sinčák, "A review of activation function for artificial neural network," in *2020 IEEE 18th World Symposium on Applied Machine Intelligence and Informatics (SAMI)*, 2020: IEEE, pp. 281-286.
- [36] A. G. Howard, "Mobilenets: Efficient convolutional neural networks for mobile vision applications," *arXiv preprint arXiv:1704.04861*, 2017.
- [37] R. Raza et al., "Lung-EffNet: Lung cancer classification using EfficientNet from CT-scan images," *Engineering Applications of Artificial Intelligence*, vol. 126, p. 106902, 2023.
- [38] C. Garbin, X. Zhu, and O. Marques, "Dropout vs. batch normalization: an empirical study of their impact to deep learning," *Multimedia tools and applications*, vol. 79, no. 19, pp. 12777-12815, 2020.
- [39] J. Zhou, A. H. Gandomi, F. Chen, and A. Holzinger, "Evaluating the quality of machine learning explanations: A survey on methods and metrics," *Electronics*, vol. 10, no. 5, p. 593, 2021.
- [40] J. Zhou, A. H. Gandomi, F. Chen, and A. Holzinger, "Evaluating the quality of machine learning explanations: A survey on methods and metrics," *Electronics*, vol. 10, no. 5, p. 593, 2021.